

# Methods for Estimating Uptake and Absorbed Dose in Tumours from $^{125}\text{I}$ Labelled Monoclonal Antibodies, Based on Scintigraphic Imaging of Mice

Anne Larsson, Lennart Johansson, Rauni Rossi Norrlund and Katrine Riklund Åhlström

From the Departments of Radiation Physics (A. Larsson, L. Johansson) and Diagnostic Radiology (R. Rossi Norrlund, K. Riklund Åhlström), Umeå University Hospital, Umeå, Sweden

Correspondence to: Dr Lennart Johansson, Radiation Physics Department, Umeå University Hospital, SE-901 85 Umeå, Sweden. Fax: + 46 90 7 85 158

Acta Oncologica Vol. 38, No. 3, pp. 361–365, 1999

Monoclonal antibodies for radioimmunotargeting are often tested in tumour bearing nude mice. In vivo determination of the uptake of the monoclonal antibody in the tumour requires quantitative scintigraphy, and this in turn requires an adequate method for subtraction of radiation from the normal tissue. For this reason, two different methods for background subtraction were evaluated, a contralateral background region of interest or an irregular one, surrounding the tumour. A pinhole collimator was used for the scintigraphy and the monoclonal antibodies were labelled with  $^{125}\text{I}$ . Furthermore, a method was developed for estimation of the mean absorbed dose in the tumour from these repeated quantitative scintigraphic measurements. This requires that the tumour mass can be accurately estimated in vivo. Finally, the results were compared with in vitro measurements of the uptake.

Received 17 April 1998

Accepted 28 September 1998

When evaluating the potential for using monoclonal antibodies (MAbs) for radioimmunotherapy (RIT), the fractional uptake of the radiolabelled MAb in the tumour is a basic parameter. The outcome of a treatment depends on a number of parameters, of which the absorbed dose in the tumour is one of the most important. The absorbed dose to the tumour depends partly on the amount of activity administered. However, the absorbed dose possible to achieve by increasing this amount is limited by the absorbed dose to normal tissues. Radiation-sensitive organs, such as the red bone marrow, set the upper level of the amount of activity administered. The tumour dose possible to achieve in man thus depends on the ratio between the absorbed dose in the tumour and the normal tissues.

Nude mice inoculated with human tumours are the most commonly used animals for evaluating and testing of new MAbs. Evaluations of this type involve assessment of the tumour uptake, which requires repeated quantitative measurements of the activity distribution in the animal. Estimation of the absorbed dose in the tumour and normal tissues in the animal model gives a rough indication of the overall characteristics of the MAb and of its potential for use in humans.

The absorbed dose in the tumour, i.e. by definition the absorbed energy per unit mass, depends on the total

number of decays taking place in the tumour and on the average amount of energy deposited in the tumour per decay. The number of decays is normally expressed as 'cumulated activity', i.e. the time-integrated activity. To a minor degree the amount of activity in the normal tissue might influence the tumour dose. The cumulated activity has been estimated in vivo from repeated quantitative scintigraphic measurements of the activity in the tumour and in the normal tissue of the mouse.

Quantitative measurements require an accurate calibration of the scintillation camera, and a correct background subtraction. In this study the tumours were situated subcutaneously in the flank of the animals. The tumour protrudes and consequently a part of it is covered with skin only, which contributes little to the background activity. In addition, the other part of the tumour represses normal tissue that contributes to a higher degree to the background activity. The amount of normal tissue included in a region of interest (ROI) of the tumour on the scintigraphic image is therefore not readily estimated. If the contribution from activity in normal tissues in the tumour ROI is assumed to be in the same order of magnitude as that in a commensurately sized background ROI located on the contralateral side of the mouse, the activity in the tumour will be underestimated. On the other hand, assum-

ing that the activity in normal tissues is negligible, the activity in the tumour will be overestimated. The accurate activity lies between these two options and, furthermore, the fraction of normal tissue activity that should be accounted for depends on the mass of the tumour. For a small tumour there is a larger contribution from normal tissues than for a large tumour. Thus in order to calculate the absorbed dose in the tumour, the absorbed fraction of energy has to be known. This parameter depends on the mass and on the geometric shape of the tumour, which vary with time, and the absorbed fraction of energy is therefore time-dependent. Furthermore, these variations in the mass also have to be considered when calculating the absorbed dose.

The aim of this study was to evaluate quantitative scintigraphy in a nude mouse tumour model using  $^{125}\text{I}$ -labelled MABs and a pinhole collimator. Another aim was to present a simple method for estimating uptake and absorbed dose in the experimental tumour and non-tumour tissue and to compare two different methods for calculating tumour activity in order to increase the accuracy in the obtained tumour/non-tumour dose ratios.

## MATERIAL AND METHODS

The investigation was performed in connection with studies of the properties of radioimmunotargeting of tumours with labelled antibodies (1–3). Thirty-seven 6-week-old female nude mice (nu/nu—BALB/C Bomholtgaard, Denmark) with  $7.5 \times 10^6$  tumour cells (HeLa Hep 2) inoculated subcutaneously in front of the right hind leg were studied. Three to 8 weeks following the tumour-cell injection, the tumour diameter varied between 4 and 15.5 mm (mean 8.4 mm). One  $^{125}\text{I}$ -labelled MAB used was directed against intracellular cytokeratin 8, named TS1, and the other MAB used was directed against membrane-bound placental alkaline phosphate, named H7. The MABs were produced by injection of hybridoma cells intraperitoneally in mice (BACB/C) and were purified using Protein A Sepharose (4). The purified MABs were labelled with  $^{125}\text{I}$  to a specific activity of approximately 80 MBq/mg MAB, using the Chloramine-T method (5).

The gamma camera (Porta Camera, General Electric, WI, USA) was equipped with a pinhole collimator, and was connected to a Star 400-evaluation system (General Electric). The pinhole had a diameter of 8.0 mm, and the distance from the pinhole to the detector was 215 mm. To obtain constant geometric conditions a special holder for the mice was fixed to the collimator 90 mm below the pinhole.

### Calibration for quantitative measurements

To be able to calculate the activity uptake in tumours in vivo, a quantitative calibration of the gamma camera was performed. The tumour was simulated by a phantom

consisting of a 10 mm-thick Plexiglas plate with holes of different sizes ( $\varnothing$ : 2, 3, 4, 5 and 6 mm) with half-spherical-shaped bottoms. Larger tumours were represented by spherical containers of Plexiglas from a phantom (Scanflex, Stockholm, Sweden) with inner diameters of 11, 13, 16 and 22 mm. The tumour phantoms were filled with a  $^{125}\text{I}$ -solution with known activity concentration,  $2.08 \text{ MBq g}^{-1} \pm 1.5\%$  (IMZ72, Amersham, Great Britain). The phantoms were weighted before and after every filling event, and the activity in each 'tumour' was determined from the mass of the used solution. A piece of plastic tape was placed over the filled holes on the small tumour phantom, to prevent the solution from leaking and evaporating. The tumour phantoms were placed on the holder and scintigraphic measurements were performed for 60 min. Each 'tumour' was covered by a ROI and the number of registered counts within each ROI was corrected according to the inverse square law to a reference point, since the 'tumour' centre points were located at different distances from the collimator. The tumour reference point, i.e. the point where the centre of the mouse tumours was assumed to be during the measurements, was located 4 mm above the mouse holder.

A correction for the attenuation in the tumours was necessary, since the calibration had to be valid for all possible mouse tumour sizes. The tumours were assumed to be spherical and the tumour tissue and the  $^{125}\text{I}$ -solution were assumed to have similar attenuation characteristics.

The escape probability,  $N_{\text{esc}}$ , for a photon emitted from the point (x, y, z) in a spherical object can be calculated as:

$$N_{\text{esc}} = \frac{1}{V} \int_{-R}^R \int_{-r}^r \int_{-y_{\text{max}}}^{y_{\text{max}}} e^{-m(y_{\text{max}}-y)} dy dx dz. \quad (1)$$

$\mu$  is the attenuation coefficient, R is the sphere radius, r is the radius of the section of the sphere at a fixed z, and  $y_{\text{max}} - y$  is the distance from the decay point to the sphere surface. To simplify the equation the exponential expression can be written as a Taylor series, and for small k,  $e^{-k} \approx 1 - k + 0.5 k^2$ . The solution to Equation (1) can then be expressed as:

$$N_{\text{esc}} \approx 1 - \frac{3}{4} \mu R + \frac{2}{5} (\mu R)^2 = 1 - \frac{3}{4} \mu \left( \frac{3m}{\rho 4\pi} \right)^{1/3} + \frac{2}{5} \mu \left( \frac{3m}{\rho 4\pi} \right)^{2/3}. \quad (2)$$

m is the tumour mass and  $\rho$  is its density, which is assumed to be  $1.0 \text{ g cm}^{-3}$ .

The effective attenuation coefficient  $\mu$  for  $^{125}\text{I}$  photon radiation in the geometry of interest was assessed by performing scintigraphic measurements on the small tumour phantom with Plexiglas plates of different thicknesses (0, 2.2, 3.9, 4.8 and 5.8 mm). The corresponding water thicknesses were calculated by multiplying the thickness of Plexiglas with the density ratio of the two materials, i.e. 1.19. The total count-rate in each image was determined and the attenuation coefficient for water was

calculated to be  $0.206 \text{ cm}^{-1}$  with exponential regression analysis.

The relation between the escape probability and the activity in the tumour,  $A_T$ , is:

$$A_T = \frac{KC_{\text{net}}}{N_{\text{esc}}t}. \quad (3)$$

$K$  is a constant,  $C_{\text{net}}$  is the number of registered net counts from the tumour (in the tumour reference point) and  $t$  is the time. The constant  $K$  depends on the number of photons escaping the tumour that are registered by the camera. Consequently it is determined by the measurement geometry, i.e. the solid angle of the pinhole as seen from the tumour, and the part of the photons attenuated in air (which can be neglected in this case). It is also dependent on the number of emitted gamma photons per decay, and the fraction of the registrations that are within the energy window. Furthermore, the attenuation in the entrance window of the detector should be accounted for.  $K$  can be calculated theoretically, but uncertainties in the pinhole diameter and in the distance between the tumour and the collimator will result in unnecessary errors. In the present study,  $A_T$ ,  $N_{\text{esc}}$  and  $C_{\text{net}}/t$  are known for all 'tumours', which made it possible to calculate  $K$  according to Equation (3).

To obtain a rough estimate of the uptake in normal tissue, a calibration was performed, simulating the mouse with a plastic bottle containing a known activity in solution. The mass of the solution was similar to that of the mice.

#### Scintigraphic measurements of mice

On day 0, the animals were injected i.p. with the  $^{125}\text{I}$ -labelled (IMS300, Amersham, Great Britain) MABs. The syringe was weighed and measured in a dose calibrator (Capintec CRC-15R, NJ, USA) before and after injection, and the activity administered to each mouse was approximately 26 MBq. The Capintec CRC-15R was calibrated with a reference  $^{125}\text{I}$ -solution (IMZ72,  $\pm 1.5\%$  Amersham, Great Britain) in the 'syringe geometry' used in all measurements. On day 1 the volume of the tumours was measured in vivo by using a microcalliper. The largest diameter (a) and the diameter perpendicular to the image plane (b) were measured and the tumour volume was estimated according to the equation  $V \approx 0.5 ab^2$ , i.e. the two smaller diameters were assumed to be equal. The anaesthetized animals were then placed on the special holder 90 mm below the pinhole collimator and the scintigraphic images were acquired in  $64 \times 64$  matrixes with 50–500 kcounts. Scintigraphic measurements were performed on the following day as well. The mice were sacrificed following the second scintigraphy, and tumours and other organs were removed, weighed and measured.

#### ROI settings

On the scintigraphic images the total number of counts was calculated within a ROI covering the tumour as visualized on the image. To correct for the counts within the tumour ROI which originate from normal tissue, an estimation of the background was necessary. Two different ROI-setting techniques were evaluated (Fig. 1):

1. A rectangular ROI covering the tumour with an equal sized 'background ROI' on the contralateral side with equal distances from the median line. The length and width of the rectangular ROIs were determined from the microcalliper measurements of the tumour volumes (the length of a pixel corresponded to 1.4 mm in the measurement geometry).
2. An irregular ROI covering the tumour, and the background derived from the count density immediately outside this ROI. The form and sizes of the irregular ROIs were determined visually.

A ROI covering the whole mouse, as visualized on the image, was also set on all images.

A tumour mass-dependent background correction was performed, according to:

$$C_{\text{net}} = C_T - C_B \frac{M_B - M_T}{M_B}. \quad (4)$$

$C_{\text{net}}$  is the tumour net counts,  $C_T$  is the counts within the tumour ROI,  $C_B$  is the counts in the background ROI, with the same area as the tumour ROI, and  $M_T$  is the mass of the tumour determined from the volume measurements.  $M_B$  is the mass of the tissue within the background ROI, and is estimated to be:

$$M_B = \frac{C_B}{C_m} M_m. \quad (5)$$

$C_m$  is the number of counts from the whole mouse (tumour excluded) and  $M_m$  is the mass of the mouse with the tumour mass subtracted. The activity in each tumour could then be calculated according to Equation (3).

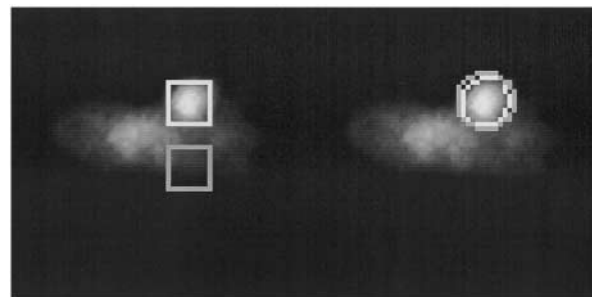


Fig. 1. Example of ROI-setting (a) method 1 and (b) method 2.

### Tumour activity measurement in vitro

To measure the activity in the tumours in vitro, a detector had to be calibrated quantitatively. A thin NaI(Tl) detector (Harshaw 757/2A, Holland) connected to a single channel analyser (Ortec 590A, TN, USA) was used for this purpose. To minimize the risk of dead time losses but still retain good statistics, four fixed calibration points at different distances from the detector were used. The dead time losses were measured to be 5% at a count rate of 8000 counts/s for this detector system. The calibration was performed with 1.0 ml  $^{125}\text{I}$  solutions with known activity (IMZ72,  $\pm 1.5\%$  Amersham, Great Britain) and care was taken to ensure that the geometry resembled the tumour measurement geometry as much as possible. At each calibration point a solution was measured 10 times at 5 min each, and the net counts were calculated by subtracting the background counts. The calibration factor in Bq min/count was calculated at each point by dividing the activity of the solution by the number of net counts per minute. The prepared mouse tumours were then measured and if the count rate was close to or in excess of 8000/s the tumour was moved to a calibration point further away from the detector. The activities were calculated, and the results were compared with the in vivo measurements from the day before sacrifice.

### Absorbed dose calculation

The mean absorbed dose rate in the tumour was calculated at different times utilizing the MIRDOSE3 program (6). Only the contribution from activity deposited in the tumour itself was considered. A small sphere with a homogeneous distribution of activity approximated the tumour. The absorbed dose from  $^{125}\text{I}$  is a function of the mass. For small masses  $< 0.75$  g, the contribution from electrons dominates completely, and the absorbed dose rate,  $\dot{D}$ , in units of Gy  $\text{kBq}^{-1} \text{day}^{-1}$  can be written:

$$\dot{D} = 2.69 \times 10^{-4} m_t^{-1}. \quad (6)$$

$m_t$  is the tumour mass in g. For larger masses, for which the photon contribution cannot be neglected, the absorbed dose rate can be approximated by:

$$\dot{D} = 2.74 \times 10^{-4} m_t^{-0.937}. \quad (7)$$

By scintigraphic measurements of the amount of activity in the tumour, and its variation from day to day, the total mean absorbed dose to the tumour can be calculated in a stepwise manner, provided that the mass of the tumour can be estimated in vivo. The mean absorbed dose to normal tissue was then estimated in a similar way.

## RESULTS AND DISCUSSION

The equation resulting from the quantitative calibration of the gamma camera is:

$$A_T = \frac{C_{\text{net}}}{t} \frac{1.46}{1 - 9.58 \cdot 10^{-2} m^{1/3} + 6.52 \cdot 10^{-3} m^{2/3}} \quad (8)$$

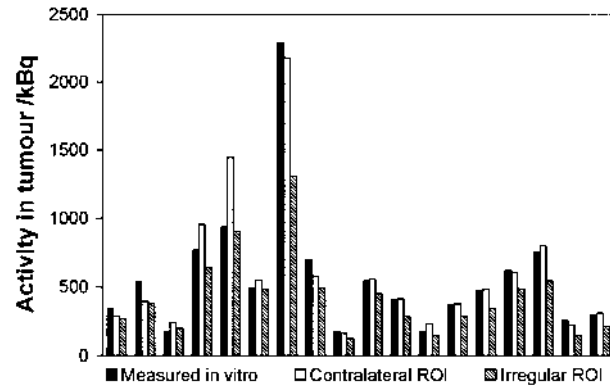


Fig. 2. Activity in tumour measured in vivo and in vitro for 18 mice. For the measurements in vivo the background has been estimated using a contralateral ROI (method 1) or an irregular ROI (method 2).

$C_{\text{net}}/t$  is the number of net counts in the tumour ROI per hour of measurement time. The error in the calibration factor, resulting partly from the uncertainty in the activity concentration of the calibration solution, is estimated to be 6%.

In a series of 37 mice the number of net counts from the tumour was estimated using methods 1 and 2 above for background correction, and the corresponding tumour activities were calculated according to equation 8. In Fig. 2 the activities from the in vivo measurements of day 2 are compared with the results from the in vitro measurements. To make it clearer, Fig. 2 is limited to include a representative sample of the total number of mice studied. It can be seen that the calculated activities from the rectangular ROI settings are closest to the measured activities for most of the mice. For all animals included in the study, the average value of the ratio of calculated to measured activity is 1.04 for method 1 and 0.77 for method 2, and the corresponding mean deviations are 17% and 24%, respectively. The estimated errors for the quantitative calibrations of the gamma camera and the scintillation detector are 6% and 5%, respectively. Consequently, method 1 gives an accurate estimation of the average value of the tumour activities. The background ROI at the contralateral side at an equal distance from the median line is an accurate representation of the background within the tumour ROI. The activities obtained using method 2 are too low, which must be the result of an overestimation of the background. This is likely to depend on scattered photons from the tumour contributing to the background just outside the tumour. Another reason can be that a large background ROI comes closer to the centre of the mouse where the count density is higher. An underestimation of the tumour size, using the visual ROI setting technique, can also be a possible explanation for the large background contribution.

The relatively large average deviations result from the uncertainties in the *in vivo* measurement method itself. Differences between the tumour centre points and the calibration reference point can result in large errors in the calculated activities. A centre point located 2 mm closer to the pinhole than the reference point would result in an error of approximately 5%. The fact that most mouse tumours were ellipsoids and not spheres may also to a minor degree contribute to the uncertainty. It is also important to note that there was an interval of 24 h between the last *in vivo* measurement and the sacrifice of the mouse. The tumour activity may have changed during that time according to the kinetic properties of the MABs used. A minor error may also arise from uncertainties in the mass determination of the tumour, since the background estimate is mass dependent. One must also consider errors resulting from the *in vitro* measurements, because of small differences between the calibration and measurement geometry.

In Fig. 3 we see the comparison between the two different weight measurement techniques. There is clearly a systematic difference between the two techniques. The ratio between the mass determined from the microcalliper measurements and the weighing is 0.77, and the reason for the difference could be:

- systematic errors in the measurement of tumour volume *in vivo* or *in vitro*;
- tumour growth between measurement *in vivo* and sacrifice;
- biophysiological processes taking place when sacrificing the mouse.

The mean absorbed dose calculated according to the method described above might be used when evaluating the biological effect of irradiation of the tumour. One additional parameter, however, is the spatial distribution of the absorbed dose within the tumour. For  $^{125}\text{I}$  this distribution reflects the distribution of the radionuclide, since the range of the Auger and conversion electrons is very short, approximately 20  $\mu\text{m}$ , for those with the highest energy of around 30 keV (7). On average, approximately 20% of the total

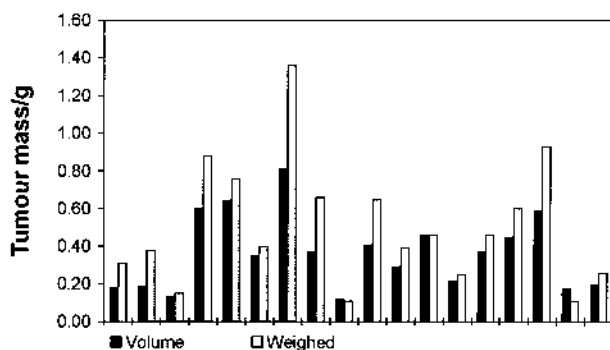


Fig. 3. Mass of the tumour measured with microcalliper *in vivo* or weighed.

energy emitted is carried by electrons with an energy of less than 5 keV, a figure that may be estimated using the MIRDOSE3 program (6). These electrons have a range of less than 1  $\mu\text{m}$  (5). Thus a prerequisite for a homogeneous distribution of the absorbed dose is that  $^{125}\text{I}$  is homogeneously distributed, not only within the tumour but also within the tumour cell.

For small tumours, especially those with a low uptake of the radiolabelled Mab, there may be a minor but significant contribution to the absorbed dose rate from photon radiation originating from normal tissues. This is the situation initially. If the dose to normal tissue from electrons and photons is calculated separately, it can be assumed that for small tumours the absorbed dose rate to the tumour from normal tissue is equal to the contribution to the dose rate to the normal tissue itself from photons. As the tumour grows larger, however, the significance of the contribution from normal tissue will decrease, and normally, since the absorbed dose rate is integrated over time, the additional contribution to the absorbed dose from decays of radionuclides found in normal tissue will be insignificant.

In the present study  $^{125}\text{I}$  was used for estimating the tumour uptake, but the method is in principle also applicable for other gamma-emitting radionuclides, such as  $^{99\text{m}}\text{Tc}$ ,  $^{111}\text{In}$ ,  $^{131}\text{I}$ ,  $^{186}\text{Re}$ , and so on. However, if the radionuclide emits photons with higher photon energies (> 250 keV) the image may deteriorate to a degree depending on which type of collimator is used. For radionuclides emitting only beta-particles, e.g.  $^{89}\text{Sr}$  and  $^{90}\text{Y}$ , scintigraphy *in vivo* with satisfying resolution is not possible. For the estimation of the absorbed dose to the tumour, it is essential to point out that the parameters presented here are valid only for  $^{125}\text{I}$ , since they depend on the type and energy of the radiation.

## REFERENCES

1. Rossi Norrlund R, Holback D, Johansson L, Hietala S-O, Riklund Åhlström K. Combinations of nonlabeled,  $^{125}\text{I}$ -labeled, and anti-idiotypic, antiplacental alkaline phosphatase monoclonal antibodies at experimental radioimmunotargeting. *Acta Radiol* 1997; 38: 1087-93.
2. Rossi Norrlund R, Ullén A, Sandström P, et al. Dosimetry of fractionated experimental radioimmunotargeting with idiotypic and anti-idiotypic anticytokeratin antibodies. *Cancer* 1997; 80: 2681-8.
3. Ullén A, Sandström P, Rossi Norrlund R, et al. Dosimetry at fractionated administration of  $^{125}\text{I}$ -labeled antibody at experimental radioimmunotargeting. *Cancer* 1997; 80: 2510-8.
4. Carlsson L, Sottrup-Jensen L, Stigbrand T. A two-site monoclonal enzyme immunoassay for pregnancy-associated  $\alpha_2$ -glycoprotein. *J Immunol Methods* 1987; 104: 73-9.
5. Greenwood F, Hunter W, Glover J. The preparation of  $^{131}\text{I}$ -labeled human growth hormone of high specific radioactivity. *J Biochem* 1963; 89: 114-23.
6. Stabin M. MIRDOSE: Personal computer software for internal dose assessment in nuclear medicine. *J Nucl Med* 1996; 37: 538-46.
7. Charlton DE. The range of high LET effects from  $^{125}\text{I}$  decays. *Radiat Res* 1986; 107: 163-71.